RESEARCH ARTICLE

Editorial Process: Submission:10/01/2025 Acceptance:06/14/2026 Published:05/22/2026

Comprehensive Pan-Cancer Bioinformatics Analysis Identifies *DHX58* as a Promising Therapeutic Target and Prognostic Biomarker Across Multiple Tumor Types

Hussam S Aziz[1,2]*, Ayoob Al-Zaalan[1]

Abstract

Background: DExH-box helicase 58 (*DHX58*/LGP2) is an innate immune regulator with a previously uncharacterized role in oncology. This study evaluates the multifaceted role of the DHX58 gene, examining its pan-cancer expression, prognostic value, and therapeutic potential across various tumor types through an extensive pan-cancer bioinformatics analysis. **Methods**: We conducted a bioinformatics analysis of *DHX58* using TCGA and GTEx data from four platforms: GEPIA2, TIMER 2.0, UALCAN, and starBase. We assessed differential expression, prognostic significance and survival outcomes, drug sensitivity, functional enrichment, genomic alterations, protein–protein interactions, and DNA methylation across 32 cancer types. **Results:** Our findings revealed that the differential expression of the *DHX58* gene across numerous cancers was context-dependent, with consistent downregulation in lung squamous cell carcinoma and upregulation in head and neck squamous cell carcinoma. Low *DHX58* expression correlated with poor survival in kidney chromophobe renal cell carcinoma, sarcoma, and skin melanoma, but with favorable outcomes in other cancers, such as colon adenocarcinoma. Notably, low *DHX58* expression was associated with increased sensitivity to birinapant and saracatinib. Genomic alterations were infrequent, and methylation patterns were largely unchanged. Functional enrichment analysis emphasized *DHX58*'s established role in innate immunity and antiviral responses, with its co-expressed genes implicated in viral defense pathways. Genomic profiling identified various alterations, including mutations and copy number variations, contributing to *DHX58* dysregulation. Protein–protein interaction mapping solidified its central role in immune signaling, while DNA methylation analysis highlighted epigenetic regulation as another layer of control. **Conclusion:** Our pan-cancer analysis reveals that *DHX58* has context-specific prognostic and predictive roles. While discrepancies between platforms exist, *DHX58* emerges as a potential biomarker in specific cancers, particularly in the context of therapies involving agents like birinapant. These findings warrant further mechanistic and clinical investigation.

Keywords: *DHX58*- Cancer- Prognostic Biomarker- Therapeutic Target- Bioinformatics- Gene Expression

Asian Pac J Cancer Prev, **27 (6)**, 2117-2127

Introduction

Cancer, a complex and heterogeneous group of diseases, remains a leading cause of morbidity and mortality worldwide, posing a significant global health challenge [1]. Characterized by uncontrolled cell growth, proliferation, and the potential to metastasize, cancer arises from a series of genetic and epigenetic alterations that disrupt normal cellular processes [2]. These alterations can affect oncogenes, tumor suppressor genes, and genes involved in DNA repair, leading to the acquisition of hallmark capabilities that enable tumor initiation, progression, and resistance to therapy [2, 3]. Understanding the intricate molecular mechanisms underlying cancer development and progression is paramount for identifying novel therapeutic targets and developing effective treatment strategies. Recent advancements in high-throughput technologies, such as genomics, transcriptomics, and proteomics, coupled with sophisticated bioinformatics tools, have revolutionized cancer research, enabling comprehensive analyses of molecular landscapes across diverse tumor types [4]. This pan-cancer approach facilitates the identification of common and distinct molecular drivers, pathways, and biomarkers that can be exploited for precision medicine. Among the myriad of genes implicated in cancer, RNA helicases, a large family of enzymes involved in various aspects of RNA metabolism, have emerged as crucial regulators of gene expression and cellular processes [5]. Their dysregulation has been linked to numerous human

*[1]Department of Medical Laboratory Technologies, College of Health and Medical Technologies, Southern Technical University, Basrah, Iraq. [2]Department of Medical Genetics, Bayan National Laboratory for Advanced Medical Diagnostics, Basrah, Iraq. *For Correspondence: hussam.aziz@stu.edu.iq*

diseases, including cancer, where they can contribute to tumorigenesis by influencing cell proliferation, survival, and metastasis [6]. DExH-box helicase 58 (*DHX58*), also known as Laboratory of Genetics and Physiology 2 (LGP2), is a member of the RIG-I-like receptor (RLR) family, primarily recognized for its critical role in innate immunity and antiviral responses [7]. LGP2 acts as a positive regulator of RIG-I and MDA5-mediated antiviral signaling, recognizing viral double-stranded RNA and facilitating the activation of downstream interferon pathways [8]. However, its precise role in cancer, particularly its context-dependent functions across different tumor types, remains to be fully elucidated. While *DHX58*'s involvement in antiviral immunity is well-established, emerging evidence suggests its potential multifaceted role in cancer. Some studies indicate a tumor-suppressive function, while others point towards an oncogenic role, highlighting the complexity and context-specificity of its actions [9, 10]. Given the critical functions of RNA helicases in cellular processes and the dual nature of *DHX58*'s reported roles, a comprehensive pan-cancer analysis is warranted to systematically investigate its expression patterns, prognostic significance, and potential as a therapeutic target across a broad spectrum of malignancies. Such an analysis can provide valuable insights into the underlying molecular mechanisms and identify specific cancer types where *DHX58* plays a pivotal role. This study aims to perform a comprehensive pan-cancer bioinformatics analysis of *DHX58* to elucidate its role as a potential therapeutic target and prognostic biomarker across multiple tumor types.

Materials and Methods

Analysis of Gene Expression in Normal Tissues

The Human Protein Atlas (HPA) (https://www.proteinatlas.org/) integrates protein and mRNA level expression profiles across organs, tissues, and individual cell types by combining multiple omics platforms including mass-spectrometry-based proteomics, antibody-dependent imaging, and transcriptomic datasets. Through its tissue and pathology modules, the HPA also delivers extensive pan-cancer insights. Using the HPA database (version 23.0), we generated an mRNA expression plot for *DHX58* in physiologically normal tissues [11].

Differential Transcriptional Profiling of DHX58 in Malignant versus Normal Tissues

To compare *DHX58* transcript abundance in tumours and their corresponding normal tissues, we interrogated four complementary platforms GEPIA2, TIMER 2.0, UALCAN, and starBase v2.0. GEPIA2 (http://gepia2.cancer-pku.cn/#analysis) integrates RNA-seq data from TCGA and GTEx, offering modules for differential-expression statistics, survival-prognosis curves, stage-wise expression plots, gene correlation matrices, and identification of expression-pattern analogues [12]. TIMER 2.0 (http://timer.cistrome.org/) extends beyond immune-infiltration analytics to include rigorous comparisons of gene expression between tumour and adjacent normal samples across multiple cancer cohorts [13]. UALCAN (http://ualcan.path.uab.edu/analysis.html) provides an interactive interface to TCGA and CPTAC datasets, enabling pan-cancer expression surveys and survival analyses for any gene of interest [14]. starBase v2.0 (http://starbase.sysu.edu.cn/panCancer.php) the Encyclopedia of RNA Interactomes (ENCORI) facilitates exploration of RNA–RNA interaction networks while furnishing pan-cancer differential-expression and survival modules [15]. In addition, the "Pathological Stage Plot" function within GEPIA2 was employed to interrogate associations between *DHX58* expression levels and tumour stage across all TCGA malignancies.

Proteomic Profiling of DHX58 Expression in Tumour and Normal Tissues

The UALCAN portal was employed to interrogate Clinical Proteomic Tumor Analysis Consortium (CPTAC) data for *DHX58* protein abundance. By querying "*DHX58*," we compared total protein levels in primary tumours versus normal tissues across the CPTAC cohorts currently available for this gene namely breast cancer, lung adenocarcinoma, head-and-neck squamous cell carcinoma, and pancreatic adenocarcinoma. Complementary protein-level information in non-malignant tissues was retrieved from the Human Protein Atlas (HPA), providing an essential reference for baseline expression patterns.

Survival Prognostic Assessment

The Gene Set Cancer Analysis (GSCA) platform (http://bioinfo.life.hust.edu.cn/GSCA/#/expression) aggregates multi-layered genomic, pharmacogenomic, and immunogenomic resources, thereby facilitating comprehensive interrogation of gene sets in oncology [16, 17]. Using this resource, we quantified the effect of *DHX58* transcript abundance on overall survival (OS) across diverse tumour cohorts. Complementary survival analyses were performed with the UCSC Xena Browser (https://xenabrowser.net/), which enables interactive exploration of TCGA and allied datasets [18]. To further validate these associations, we employed GEPIA2; its "Survival Map" module generated an OS importance heat-map for *DHX58* spanning all TCGA cancer types. Lastly, pan-cancer survival correlations were corroborated via the starBase v2.0 / ENCORI platform, which provides integrated analyses of RNA expression and clinical outcomes. Across all databases, statistical significance was adjudged at a log-rank $P < 0.05$. Finally, we integrated survival datasets from all platforms to interrogate the prognostic significance of *DHX58* mRNA expression across the full spectrum of malignancies under study.

Drug-Sensitivity Analysis

To delineate the clinical implications of aberrant *DHX58* expression and evaluate its utility as a predictive biomarker for pharmacological screening, we performed a drug-sensitivity analysis via the Gene Set Cancer Analysis (GSCA) platform. Half-maximal inhibitory concentration (IC_{50}) values for 481 chemotherapeutic agents were obtained, together with corresponding RNA-seq profiles, from the Cancer Therapeutics Response Portal (CTRP) dataset housed within GSCA. Pearson correlation

coefficients were then computed to quantify associations between *DHX58* transcript abundance and compound IC_{50}, with a false-discovery-rate adjustment applied to control for multiple testing. A negative correlation signifies that elevated *DHX58* expression coincides with decreased drug sensitivity (i.e., potential resistance), whereas a positive correlation indicates heightened sensitivity.

Functional Enrichment Profiling of DHX58

The Enrichr web platform (https://maayanlab.cloud/Enrichr/) [19, 20] was queried to retrieve the 100 genes exhibiting the strongest co-expression with *DHX58*, as defined by the ARCHS4 RNA-seq gene–gene co-expression matrix. Enrichment analysis was undertaken for the aforementioned set of 100 *DHX58*-co-expressed genes to elucidate their prospective functional roles across malignancies. Gene Ontology (GO) over-representation testing encompassed the biological process, molecular function, and cellular component domains, while pathway analyses incorporated annotations from KEGG, WikiPathways, and Reactome. All calculations were executed with Enrichr, adopting a significance threshold of $P < 0.05$. Resulting GO terms and pathway enrichments were visualised as dot-plots generated in R (v4.2.1) using the ggplot2 package [21] within RStudio Desktop (v2022.7.0.548).

Cancer-Associated Fibroblast (CAF) Infiltration Profiling

The TIMER 2.0 platform was used to delineate the association between *DHX58* transcript abundance and cancer-associated fibroblast (CAF) infiltration across 32 TCGA tumour types. Within the "Immune-Gene" module, CAF density was quantified using the EPIC algorithm, and partial Spearman correlation coefficients were calculated with tumour-purity adjustment. Correlations achieving a two-sided $P < 0.05$ were regarded as statistically significant.

Genomic Alteration Profiling of DHX58

Genomic perturbations involving *DHX58* were characterised with cBioPortal for Cancer Genomics (https://www.cbioportal.org/) [22]. Within the TCGA Pan-Cancer Atlas cohort we queried "*DHX58*," selecting molecular profiles for point mutations and copy-number alterations. The Cancer Types Summary panel enumerated the incidence of mutation, amplification, deep deletion and composite events across all TCGA entities, whereas the Mutations module detailed the distribution and protein-level consequences of each variant. To contextualise these findings, mutation prevalence was also extracted from the Gene_Mutation module of TIMER 2.0 (https://timer.cistrome.org/) , providing a tumour-by-tumour overview of *DHX58*-altered cases. This integrative approach affords a comprehensive view of *DHX58* genetic alterations across the cancer spectrum.

Protein–Protein Interaction Profiling of DHX58

Protein–protein interaction (PPI) mapping for *DHX58* was performed with STRING v12 (https://string-db.org/) [23]. Parameters were set to include all evidence channels, an interaction score threshold of 0.15, and a maximum of 100 interactors, yielding both direct (physical) and indirect (functional) associations. To validate physical PPIs, we queried BioGRID v4.4.247 (https://thebiogrid.org), an open-access repository that catalogues experimentally supported protein, genetic, and chemical interactions as well as post-translational modifications [24]. Interactomes were visualized in the BioGRID 'Network' module using a concentric-circle layout. Finally, overlap between the STRING- and BioGRID-derived interactors was determined with Venny 2.1.0 (https://bioinfogp.cnb.csic.es/tools/venny/) to identify PPIs for *DHX58* that are corroborated in the literature [25-27].

DNA Methylation Analysis

The DNMIVD database (http://119.3.41.228/dnmivd/index/) is an interactive platform that aggregates DNA-methylation data from the Gene Expression Omnibus (GEO) and The Cancer Genome Atlas (TCGA) [25, 26]. Using this resource, we retrieved *DHX58* promoter-methylation profiles for all TCGA cohorts. Differential methylation between tumour and matched normal specimens was assessed with an independent Student's t-test; tumours were deemed significantly altered when both the absolute β-value difference exceeded 0.20 and the adjusted p-value was below 0.05. In cases exhibiting aberrant promoter methylation, we further evaluated the relationship between methylation status and *DHX58* transcript abundance in primary tissues via Pearson and Spearman correlation analyses, applying stringent thresholds ($|R| > 0.10$; $p < 0.05$) to capture biologically relevant associations.

Results

Analysis of Gene Expression in Normal Tissues

Functional Annotation and Tissue Level Distribution of *DHX58* within the Human Protein Atlas (HPA) framework, we examined the Functional Annotation of the Mammalian Genome (FANTOM5) dataset alongside the GTEx project and a hybrid Consensus dataset that integrates HPA and GTEx outputs. This comparative analysis demonstrated pronounced *DHX58* transcription in multiple anatomical sites including the salivary gland, spleen, liver, ovary, lymph node, bone marrow, and thymus (Figure 1A;). Consistent with these widespread signals, the gene exhibits minimal tissue restriction, as reflected by a Tau specificity score of 0.28. Single-cell expression profiling indicates that *DHX58* displays low cell-type specificity (Figure 1B). Complementary comparative-genomic inspection in the UCSC Genome Browser reveals only moderate evolutionary conservation of *DHX58* across vertebrate lineages (Figure 1C).

Differential Transcriptional Profiling of DHX58 in Malignant versus Normal Tissues

For the differential expression analysis of *DHX58* in various cancer types compared to normal tissues, we used the GEPIA2, TIMER2.0, UALCAN, and starBase databases. According to GEPIA2 database analysis revealed downregulation of the *DHX58* gene in tumor tissues of Lung Squamous Cell Carcinoma (LUSC),

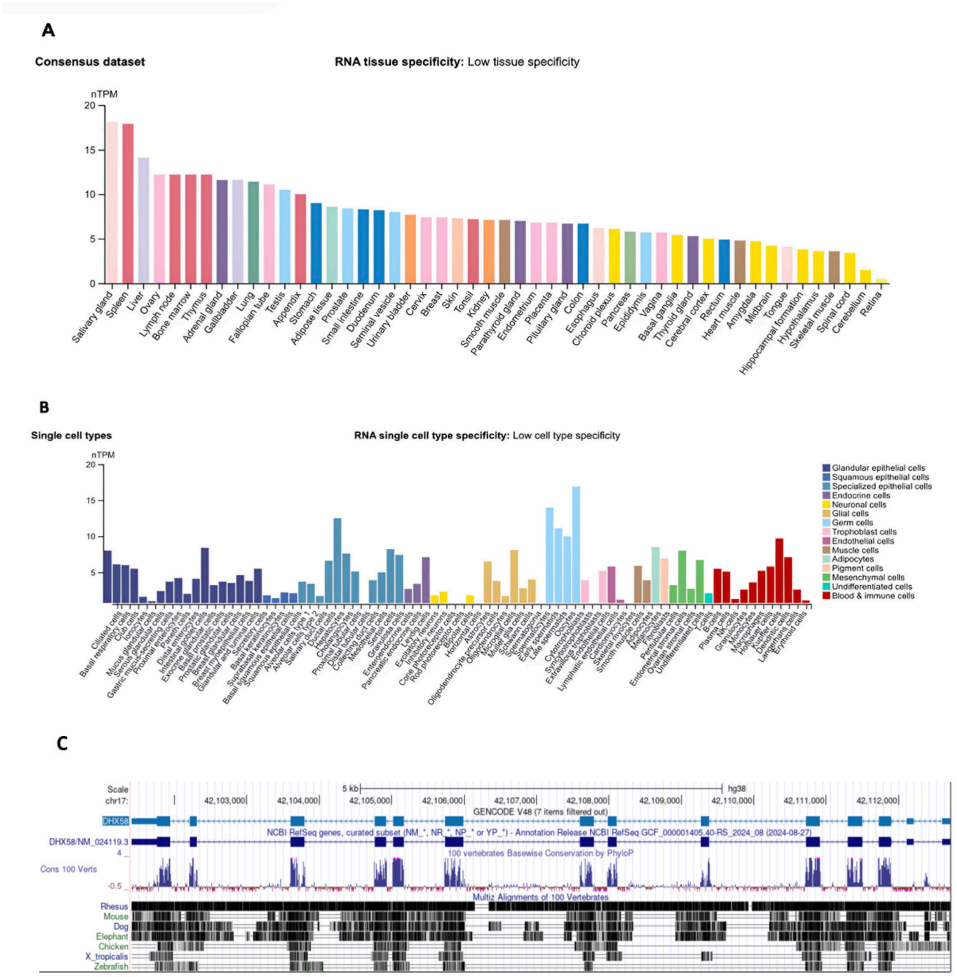

Figure 1. Comprehensive landscape of *DHX58* expression and evolutionary conservation. (A) Consensus tissue-level expression of *DHX58* derived from the Human Protein Atlas (HPA) and GTEx datasets. (B) Single-cell *DHX58* expression profiles curated by the HPA. (C) Comparative analysis of *DHX58* genomic conservation across vertebrate species.

Ovarian Serous Cystadenocarcinoma (OV), Testicular Germ Cell Tumors (TGCT), and Uterine Carcinosarcoma (UCS). Conversely, it exhibited upregulation in Diffuse Large B-Cell Lymphoma (DLBC), Head and Neck Squamous Cell Carcinoma (HNSC), Acute Myeloid Leukemia (LAML), Pancreatic Adenocarcinoma (PAAD), and Thymoma (THYM) (Figure 2A, Table 1).

The TIMER2.0, *DHX58* mRNA expression exhibited a notable decrease in cancerous tissues across multiple cancer types when compared to their respective healthy counterparts. Specifically, tumor tissues of LUSC (p-value <0.001), and Lung Adenocarcinoma (LUAD) (p-value <0.05), displayed a significant downregulation in *DHX58* expression. Conversely, elevated expression of *DHX58*

Table 1. Summary of *DHX58* Expression Patterns across Diverse Tumor Types Compiled from Multiple Independent Datasets

Database	*DHX58* expression pattern	
	Upregulation	Downregulation
GEPIA2	DLBC-HNSC-LAML-PAAD-THYM	LUSC-OV-TGCT-UCS
TIMER2.0	BRCA-CHOL- HNSC-KIRP-LIHC	LUAD- LUSC
UALCAN	BLCA-BRCA-CHOL-ESCA-HNSC-KIRP-STAD	KICH- LUSC
starBase	HNSC-KIRP-BRCA-BLCA-CHOL-KIRC-READ-STAD-ESCA	KICH-LUSC
Common	HNSC	LUSC

Diffuse Large B-cell Lymphoma (DLBC), Head and Neck Squamous Cell Carcinoma (HNSC), Acute Myeloid Leukemia (LAML), Pancreatic Adenocarcinoma (PAAD), Thymoma (THYM), Lung Squamous Cell Carcinoma (LUSC), Ovarian Serous Cystadenocarcinoma (OV), Testicular Germ Cell Tumors (TGCT), Uterine Carcinosarcoma (UCS), Breast Invasive Carcinoma (BRCA), Cholangiocarcinoma (CHOL), Kidney Renal Papillary Cell Carcinoma (KIRP), Liver Hepatocellular Carcinoma (LIHC), Lung Adenocarcinoma (LUAD), Bladder Urothelial Carcinoma (BLCA), Esophageal Carcinoma (ESCA), Stomach Adenocarcinoma (STAD), Kidney Chromophobe (KICH), Kidney Renal Clear Cell Carcinoma (KIRC), and Rectum Adenocarcinoma (READ)

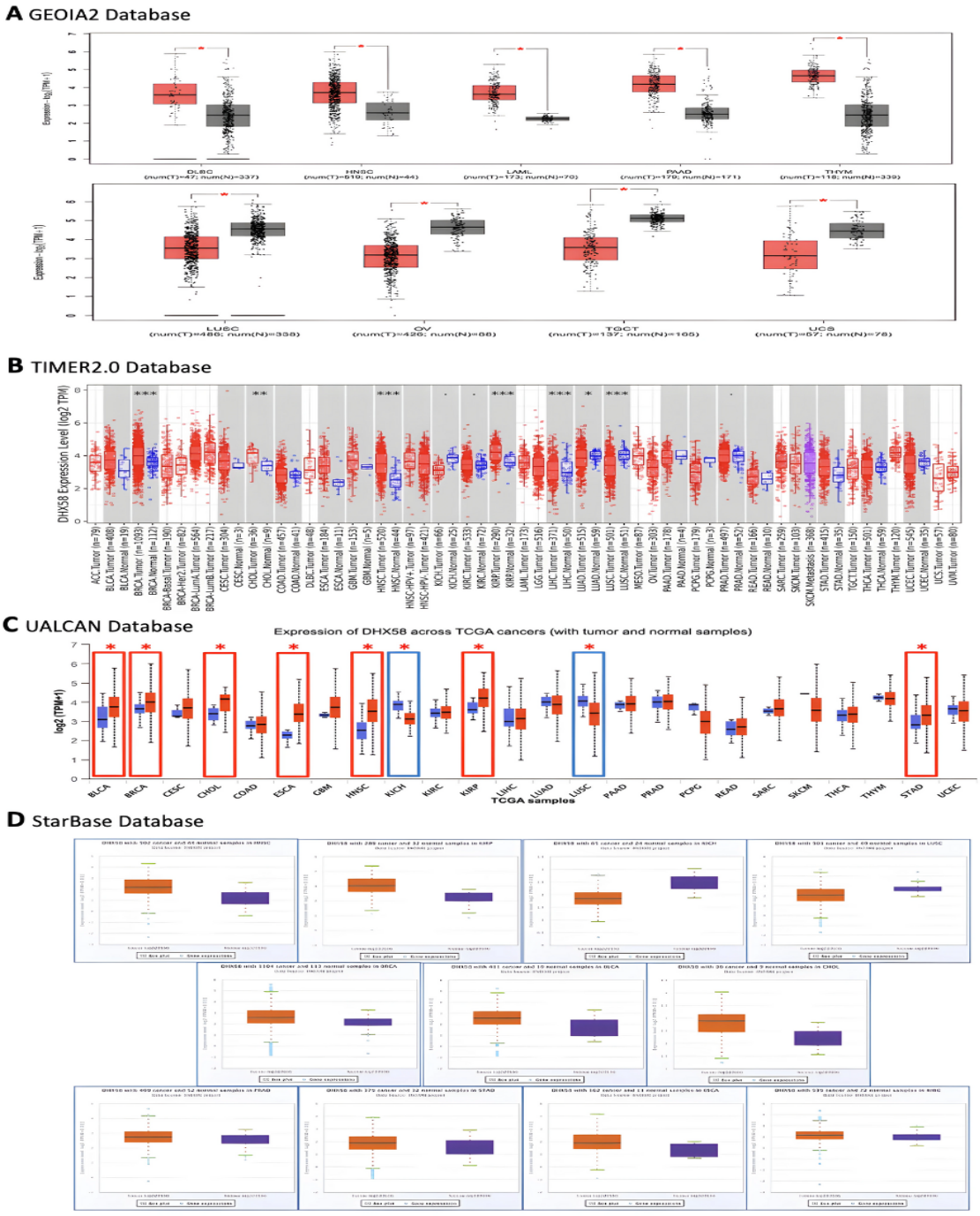

Figure 2. Differential Transcriptional landscape of *DHX58* across TCGA tumour cohorts interrogated via multiple bioinformatics resources. (A) Box-plot depicting *DHX58* mRNA abundance in tumour specimens versus matched TCGA normal and GTEx tissues, generated with GEPIA2 (* $P < 0.05$). (B) DHX58 expression profiles across diverse cancer types visualised through TIMER 2.0 (* $P < 0.05$; ** $P < 0.01$; *** $P < 0.001$). (C) Pan-cancer overview of DHX58 transcriptional activity obtained from the UALCAN portal (* $P < 0.05$). (D) starBase v2.0 analysis highlighting tumour-specific up- and down-regulation of DHX58; orange and blue box-plots represent malignant and normal tissues, respectively (FDR < 0.05).

was observed in Breast Invasive Carcinoma (BRCA), HNSC, Kidney Renal Papillary Cell Carcinoma (KIRP), and Liver Hepatocellular Carcinoma (LIHC) (p-value <0.001), as well as Cholangiocarcinoma (CHOL) (p-value <0.01) when compared to normal tissues (Figure 2B, Table 1). Findings from the UALCAN database supported the downregulation of *DHX58* in Kidney Chromophobe (KICH), and LUSC, while upregulation was observed in Bladder Urothelial Carcinoma (BLCA), BRCA, Cholangiocarcinoma (CHOL), Esophageal Carcinoma (ESCA), HNSC, Kidney Renal Papillary Cell Carcinoma (KIRP), and Stomach Adenocarcinoma (STAD) (p-value

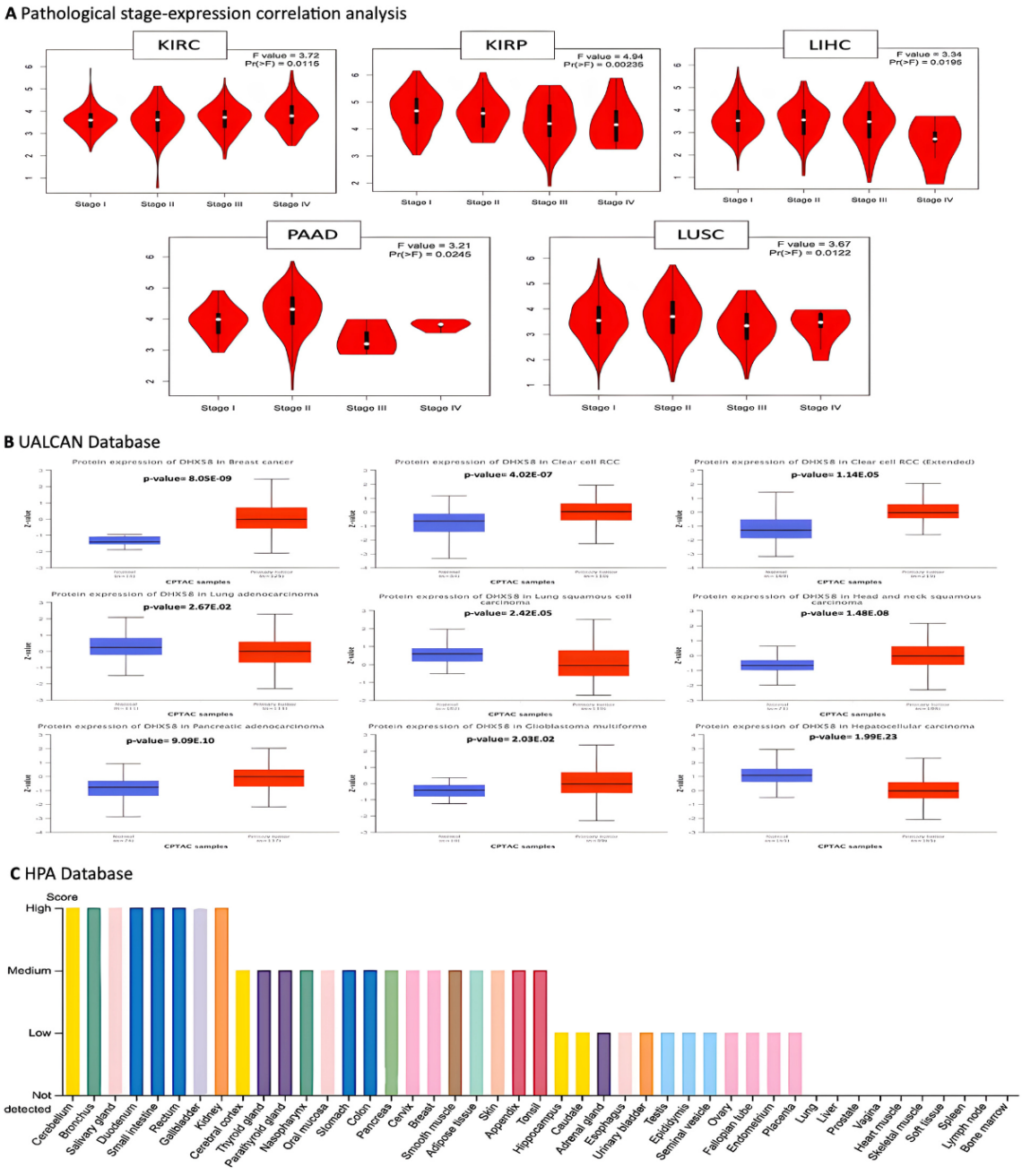

Figure 3. Stage- and Tissue-Specific Expression patterns of *DHX58*. (A) Transcript levels of *DHX58* across pathological stages for selected tumour types. (B) UALCAN-derived box-plot comparing DHX58 protein abundance in primary tumours versus matched normal tissues. (C) Pan-cancer overview of DHX58 protein expression in tumour specimens obtained from the Human Protein Atlas (HPA).

< 0.05) (Figure 2C, Table 1). Additionally, insights derived from the starBase database further validated the downregulated expression of *DHX58* in tumor tissues of Kidney Chromophobe (KICH), and LUSC, while HNSC, KIRP, BRCA, BLCA, CHOL, Kidney Renal Clear Cell Carcinoma (KIRC), BRAD, Stomach Adenocarcinoma (STAD), and Esophageal Carcinoma (ESCA) exhibited higher expression levels relative to normal tissues, with FDR < 0.05 (Figure 2D, Table 1). Cross-comparison of GEPIA2, TIMER 2.0, UALCAN, and starBase datasets (Table 1) pinpointed tumour entities in which *DHX58* is significantly dysregulated. Transcript levels were uniformly down-regulated in lung squamous cell carcinoma (LUSC), whereas pronounced over-expression was confined to head-and-neck squamous cell carcinoma (HNSC). Stage-stratified analyses further demonstrated significant associations between *DHX58* mRNA abundance and pathological stage in KIRC, KIRP, LIHC, PAAD, and LUSC ($P < 0.05$; Figure 3A).

Proteomic Profiling of DHX58 Expression in Tumor and Normal Tissues

Using the UALCAN portal, we compared *DHX58* protein abundance in primary tumors with that in matched normal solid tissues. *DHX58* levels were significantly higher in normal samples than in tumor specimens from

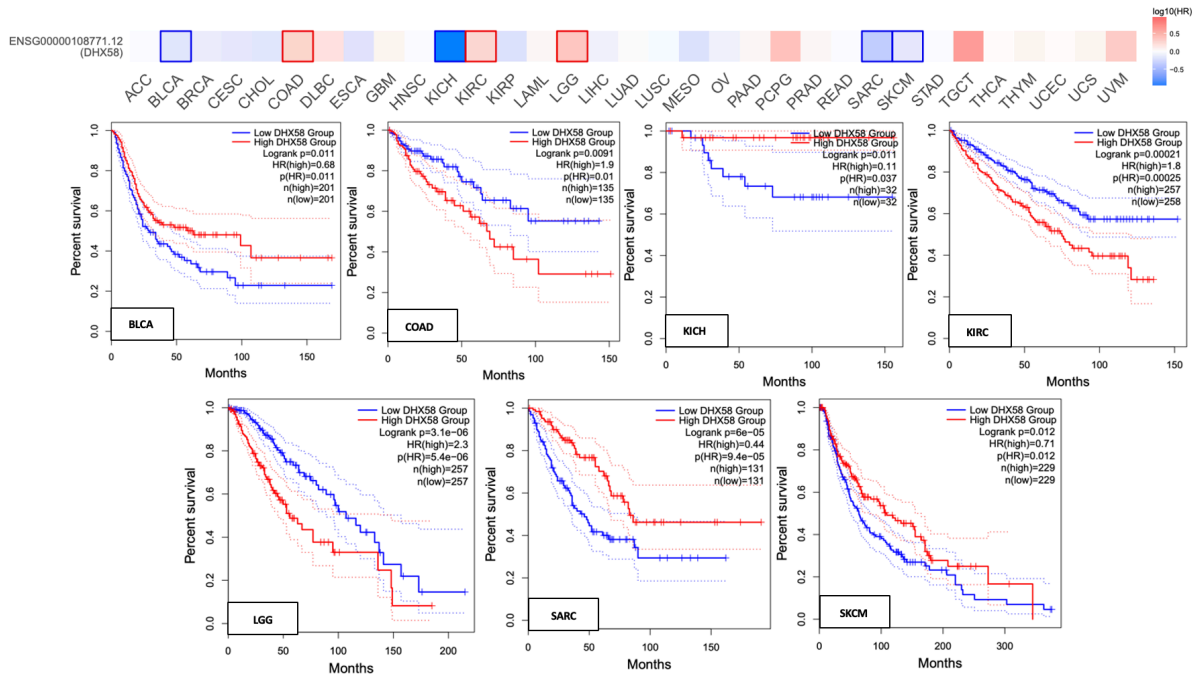

Figure 4. Association between *DHX58* Transcript Abundance and Patient Survival. Generated with GEPIA2 illustrating overall-survival (OS) differences between high- and low-DHX58 expression cohorts across TCGA tumour types.

lung adenocarcinoma (LUAD), lung squamous cell carcinoma (LUSC) and hepatocellular carcinoma (LIHC). Conversely, the protein was markedly up-regulated in primary tumors relative to normal tissues in breast cancer (BRCA), clear-cell renal cell carcinoma (KIRC; standard and extended cohorts), head-and-neck squamous cell carcinoma (HNSC), pancreatic adenocarcinoma (PAAD) and glioblastoma multiforme (GBM) (Figure 3B). Analysis of immunohistochemical data in the Human Protein Atlas (HPA) showed markedly elevated *DHX58* protein abundance in normal tissues, including the cerebellum, bronchus, salivary gland, duodenum, small intestine, rectum, gallbladder, and kidney (Figure 3C). Clarifying the biological ramifications of these baseline expression patterns is essential, as *DHX58* may modulate signaling pathways that underpin tumour initiation and progression.

Survival Prognostic Assessment

On the basis of the observed dysregulation of *DHX58* in multiple malignancies, we hypothesized that its expression might influence patient survival. Accordingly, we interrogated GEPIA2, starBase, and GSCA to assess associations between *DHX58* transcript abundance and overall survival (OS). In GEPIA2, cases were dichotomized into high- and low-expression cohorts using the cohort-specific median *DHX58* mRNA level, after which OS was evaluated. Reduced *DHX58* expression correlated with inferior OS in bladder carcinoma (BLCA; P = 0.011, HR = 0.68), kidney chromophobe (KICH; P = 0.037, HR = 0.11), sarcoma (SARC; P = 9.4e-05, HR = 0.44) and skin cutaneous melanoma (SKCM; P = 0.012, HR = 0.71). Conversely, elevated *DHX58* expression predicted improved OS in colon adenocarcinoma (COAD; P = 0.01, HR = 1.9), clear-cell renal carcinoma (KIRC; P = 0.00025, HR = 1.8) and lower-grade glioma (LGG; P = 5.4e-06, HR = 2.3) (Figure 4; Table 2).

Within the GSCA, reduced *DHX58* transcript abundance correlated with inferior overall survival (OS) in BRCA (P = 0.0013), ESCA (P = 0.0049), KICH (P = 0.0087), LIHC (P = 0.0039), SARC (P = 5e.04) and SKCM (P = 0.011). In contrast, elevated *DHX58* expression predicted poorer OS in COAD (P = 0.0018), KIRC (P = 0.00068) and LGG (P = 6.7e.06) (Figure 5A; Table 2). Parallel analyses in the starBase v2.0 corroborated these trends. Low *DHX58* expression was linked to diminished OS in BRCA (P = 0.033, HR = 0.70), SKCM (P = 0.040, HR = 0.75), KICH (P = 0.014, HR = 0.12), SARC (P =

Table 2. Association between aberrant *DHX58* Expression and Adverse Prognosis Across TCGA Cohorts

Overall survival (OS)	Upregulation with poor prognosis	Downregulation with poor prognosis
GEPIA2	COAD-KIRC-LGG	BLCA-KICH-SARC-SKCM
GSCA	COAD- KIRC-LGG	BRCA-ESCA-KICH-LIHC-SARC- SKCM
starBase	COAD-KIRC-LGG	BRCA-SKCM-KICH-SARC-BLCA-ESCA
Common	COAD-KIRC-LGG	KICH- SARC- SKCM

Colon Adenocarcinoma (COAD), Kidney Renal Clear Cell Carcinoma (KIRC), Brain Lower Grade Glioma (LGG), Bladder Urothelial Carcinoma (BLCA), Kidney Chromophobe (KICH), Sarcoma (SARC), Skin Cutaneous Melanoma (SKCM), Breast Invasive Carcinoma (BRCA), Esophageal Carcinoma (ESCA), and Liver Hepatocellular Carcinoma (LIHC).

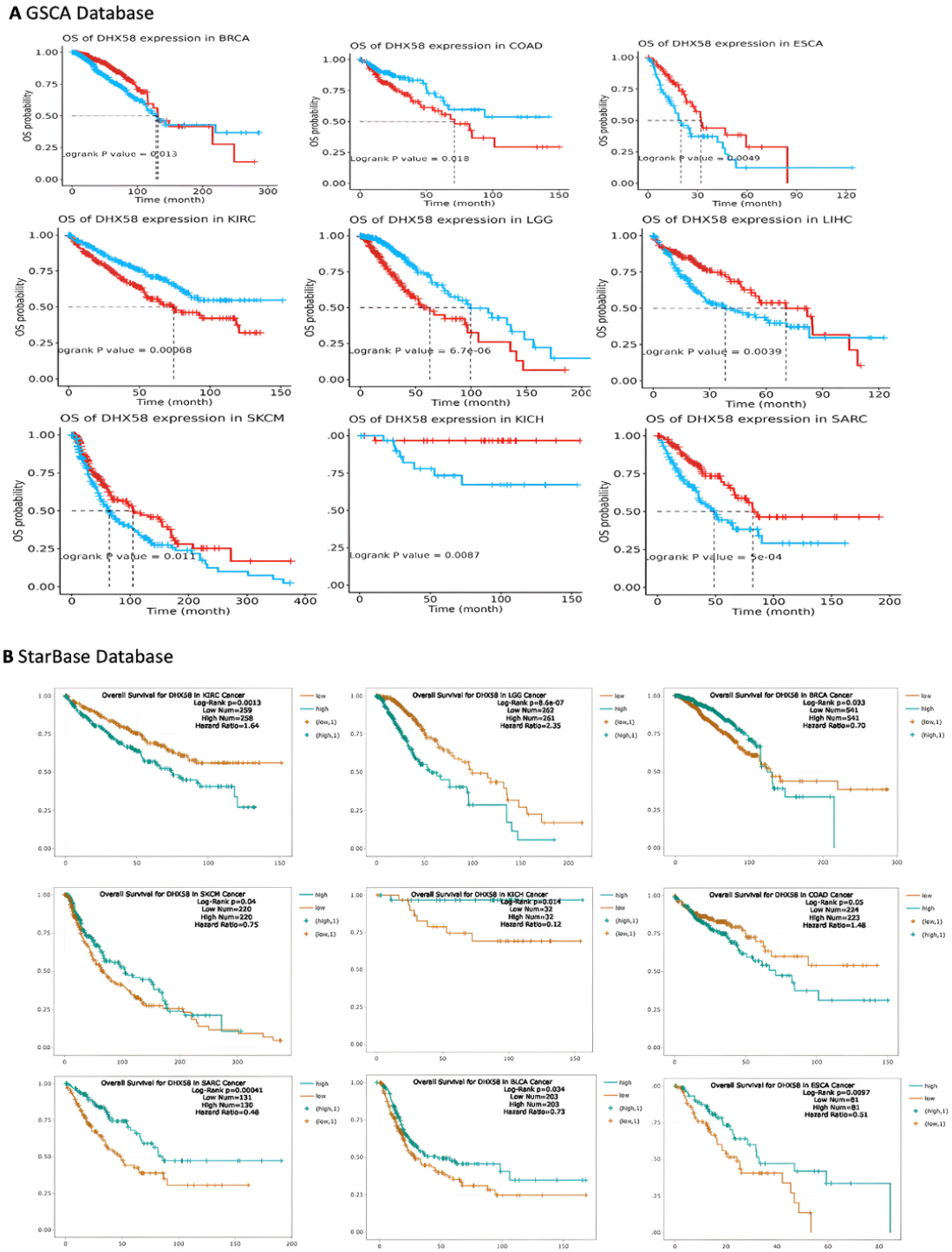

Figure 5. Prognostic Impact of *DHX58* expression on Overall Survival (OS). (A) Kaplan–Meier OS analyses generated with the Gene Set Cancer Analysis (GSCA) platform. (B) Corresponding OS curves derived from the starBase v2.0 database.

0.00041, HR = 0.48), BLCA (P = 0.034, HR = 0.73) and ESCA (P = 0.0097, HR = 0.51). Conversely, *DHX58* up-regulation was associated with adverse OS in KIRC (P = 0.0013, HR = 1.64), LGG (P = 8.6e.07, HR = 2.35) and COAD (P = 0.050, HR = 1.48) (Figure 5B; Table 2). Consolidated survival-prognosis analyses indicated that low *DHX58* expression predicted poorer overall survival in KICH, SARC, and SKCM, whereas high *DHX58* transcript levels were associated with unfavourable outcomes in COAD, KIRC, and LGG (Table 2).

Drug-Sensitivity Analysis

Interrogation of the CTRP dataset demonstrated that tumours exhibiting low *DHX58* transcript levels were markedly more responsive to the SMAC mimetic birinapant and the Src inhibitor saracatinib ($r < -0.2$; FDR < 0.001; Supplementary Figure 1A).

Functional Enrichment Profiling of DHX58

Our comprehensive enrichment analysis demonstrates that the identified genes play a pivotal role in orchestrating cellular defense mechanisms, with a pronounced emphasis on the innate immune system. The Gene Ontology (GO) analysis provided granular insights into their functions. For Biological Processes, the most significant terms included "Defense Response to Virus" and "Negative Regulation of Viral Process," alongside signaling pathways like "Interleukin-27-Mediated Signaling," indicating a specialized function in controlling viral replication and modulating immune communication. In the Molecular Function domain, terms such as "CARD Domain Binding" and "Double-Stranded RNA Binding" were prominent, highlighting the genes' role in the direct recognition of pathogen-associated molecular patterns. Consistent with these functions, the Cellular Component analysis localized these genes to critical immune compartments like the "Phagocytic Vesicle," "Endosome Lumen," and "Tertiary Granule Lumen." Building on these functional annotations, our pathway analysis across KEGG, Reactome, and WikiPathways databases revealed the specific systemic pathways where these genes operate. The analysis identified highly significant enrichment in overarching immune pathways, including the "Innate Immune System" and "Cytokine Signaling in Immune System." More specifically, the genes were implicated in defense pathways against a range of pathogens, with "Immune Response to Tuberculosis" and "Type I Interferon Signaling" being among the top hits. Furthermore, their involvement in numerous viral response pathways, such as those for Influenza, Measles, SARS-CoV-2, and Hepatitis C, was clearly established. These integrated results (Supplementary Figure 2) strongly suggest that the studied genes are central components of the innate immune signaling cascade, crucial for mounting an effective defense against a wide spectrum of viral and bacterial threats.

Cancer-Associated Fibroblast (CAF) Infiltration Profiling

To delineate the relationship between *DHX58* transcript abundance and cancer-associated fibroblast (CAF) infiltration, we queried the TIMER 2.0 "Immune-Gene" module and applied the EPIC deconvolution algorithm with tumour-purity adjustment. The resulting heat-map displays partial Spearman correlation coefficients (ρ) for 32 TCGA entities, highlighting statistically significant associations ($P < 0.05$). Positive correlations were detected in COAD, LGG, LUSC, PAAD, PRAD, READ, STAD, TGCT, and THCA, shown as red cells. Negative correlations emerged in BLCA, BRCA-LumA, KIRP, MESO, PCPG, SARC, SKCM, and SKCM-metastasis, depicted in blue. The remaining tumour types exhibited no significant association (Supplementary Figure 3 A). Representative scatter-plots are provided in Supplementary Figure 3B. Collectively, these data suggest that *DHX58* expression may modulate CAF abundance in a cancer-type-specific manner, with particularly notable effects in breast and selected urogenital malignancies.

Genomic Alteration Profiling of DHX58

Using cBioPortal, we surveyed *DHX58* genomic alterations across 32 TCGA tumour types. The highest overall alteration rates occurred in UCEC (4.54 %), STAD (4.09 %) and ESCA (2.75 %). Stratified by alteration class, UCEC exhibited the greatest mutation burden (4.16 %), whereas ACC and ESCA showed the largest proportions of deep deletions (2.2 %) and amplifications (2.75 %), respectively; all remaining cancers displayed alteration frequencies below 2 % (Supplementary Figure 4A). In total, 88 *DHX58* variants were catalogued, comprising 77 missense substitutions, eight truncating events and three splice-site changes, dispersed across both annotated domain and non-domain regions of the protein (Supplementary Figure 4B). Independent interrogation with TIMER 2.0 confirmed the greatest prevalence of *DHX58* mutations in UCEC (21/531 cases), COAD (10/406) and STAD (10/439) (Supplementary Figure 4C).

Protein–Protein Interaction Profiling of DHX58

Interrogation of the STRING v12 interactome identified the 100 proteins with the strongest predicted physical or functional connectivity to *DHX58* (Supplementary Figure 5A). Subsequent curation with BioGRID v4.4.247 uncovered 24 experimentally validated physical interactors: five genes (*APP, CDKN2AIP, STAU1, AP2B1, XRN2*) derived exclusively from high-throughput (HTP) screens; twelve genes (*EIF2AK2, TRAF3, USP21, TRAF5, RNF135, IFIH1, TRAF6, SLFN11, TRIM25, TRAF2, TRIM14, DDX58*) reported in low-throughput (LTP) studies; and seven genes (*EIF6, DHX30, NKRF, IFI16, STAU2, DICER1, AGO2*) supported by both HTP and LTP evidence (Supplementary Figure 5B). Intersecting the STRING-derived network with the BioGRID dataset via Venny 2.1 highlighted 12 interactors (*EIF2AK2, TRIM25, RNF135, TRIM14, IFI16, DHX30, TRAF6, XRN2, TRAF3, DDX58, IFIH1, DICER1*) that are corroborated by literature-based evidence (Supplementary Figure 5C).

DNA Methylation Analysis

When utilizing the DNMIVD database to explore the methylation pattern of the *DHX58* gene's promoter across 23 distinct cancer types, no significant hypermethylation or hypomethylation was identified in the promoter region of the *DHX58* gene in any cancer type (all adjusted p-values > 0.05 and |beta difference| < 0.2). Moreover, the results of the correlation study revealed several notable inverse associations between the level of methylation in the promoter region and the expression level of the *DHX58* gene in multiple cancer types. Specifically, a significant negative correlation was observed in UCEC (Pearson R = −0.517105, Pearson p-value = 5.08e-33; Spearman R = −0.414262, Spearman p-value = 1.26e-20), THCA (Pearson R = −0.719025, Pearson p-value = 0; Spearman R = −0.692332, Spearman p-value = 0), and GBM (Pearson R = −0.430582, Pearson p-value = 3.83e-04; Spearman R = −0.360943, Spearman p-value = 0.0033). These findings suggest a potential inverse relationship between promoter methylation and *DHX58* expression in certain cancer types, highlighting the need for further experimental validation.

Discussion

The present study aimed to comprehensively analyze the role of *DHX58* as a potential therapeutic target and prognostic biomarker across multiple tumor types, utilizing various bioinformatics platforms. Our findings reveal a complex and multifaceted involvement of *DHX58* in cancer biology, encompassing differential expression, prognostic significance, drug sensitivity, functional enrichment, genomic alterations, protein-protein interactions, and DNA methylation patterns.

DHX58 exhibited differential expression patterns across various cancer types compared to normal tissues. Specifically, downregulation was observed in Lung Squamous Cell Carcinoma (LUSC), Ovarian Serous Cystadenocarcinoma (OV), Testicular Germ Cell Tumors (TGCT), and Uterine Carcinosarcoma (UCS) based on GEPIA2 analysis. Conversely, upregulation was noted in Diffuse Large B-Cell Lymphoma (DLBC), Head and Neck Squamous Cell Carcinoma (HNSC), Acute Myeloid Leukemia (LAML), Pancreatic Adenocarcinoma (PAAD), and Thymoma (THYM) (Figure 2A, Table 1). These findings were largely corroborated by TIMER 2.0, UALCAN, and starBase databases, highlighting the consistent dysregulation of *DHX58* in specific malignancies. Notably, LUSC consistently showed downregulation, while HNSC consistently showed upregulation across multiple platforms (Table 1) Beyond transcriptional changes, proteomic analysis via UALCAN and Human Protein Atlas (HPA) revealed elevated *DHX58* protein levels in normal tissues compared to tumor specimens in LUAD, LUSC, and LIHC. Conversely, upregulation was observed in primary tumors of BRCA, KIRC, HNSC, PAAD, and GBM (Figure 3B, 3C). This discrepancy between mRNA and protein expression in some cancers suggests post-transcriptional regulatory mechanisms that warrant further investigation. Prognostic assessment demonstrated that *DHX58* expression significantly influences patient survival, albeit with context-dependent effects. Reduced *DHX58* expression correlated with inferior overall survival (OS) in BLCA, KICH, SARC, and SKCM, while elevated expression predicted improved OS in COAD, KIRC, and LGG [16, 17]. These associations were consistent across GEPIA2, GSCA, and starBase platforms, underscoring the potential of *DHX58* as a prognostic biomarker.

Drug sensitivity analysis indicated that low *DHX58* transcript levels were associated with increased responsiveness to the SMAC mimetic birinapant and the Src inhibitor saracatinib [16, 17]. This suggests that *DHX58* expression could serve as a predictive biomarker for therapeutic response, guiding personalized treatment strategies.

Functional enrichment profiling revealed that *DHX58*-co-expressed genes are primarily involved in cellular defense mechanisms, particularly the innate immune system, with a strong emphasis on viral response pathways. Key terms included "Defense Response to Virus," "Negative Regulation of Viral Process," "CARD Domain Binding," and "Double-Stranded RNA Binding." Pathway analyses implicated *DHX58* in the "Innate Immune System" and "Cytokine Signaling in Immune System," as well as specific viral response pathways for Influenza, Measles, SARS-CoV-2, and Hepatitis C [19, 20]. These findings align with the known role of *DHX58* (also known as LGP2) as a DExH-box helicase involved in innate immunity and antiviral responses [11]. Genomic alteration profiling showed varying rates of *DHX58* alterations across TCGA tumor types, with the highest overall alteration rates in UCEC, STAD, and ESCA. Mutations, deep deletions, and amplifications were observed, with UCEC exhibiting the greatest mutation burden [22]. Protein-protein interaction (PPI) mapping identified numerous interactors, with several experimentally validated physical interactors such as EIF2AK2, TRAF3, and IFIH1, further supporting *DHX58*'s role in immune signaling pathways [23, 24]. Lastly, DNA methylation analysis revealed inverse correlations between *DHX58* promoter methylation and its expression in certain cancer types (UCEC, THCA, and GBM) points to epigenetic regulation as another layer of control. DNA methylation in promoter regions is generally associated with gene silencing [24]. Therefore, hypomethylation leading to increased *DHX58* expression could contribute to its oncogenic role in some contexts, while hypermethylation leading to decreased expression might contribute to its tumor suppressive role in others. This highlights the epigenetic landscape as a potential target for therapeutic intervention aimed at modulating *DHX58* expression.

In conclusion, this comprehensive pan-cancer bioinformatics analysis has elucidated the intricate and context-dependent role of *DHX58* in various malignancies. Our findings demonstrate that *DHX58* exhibits differential expression patterns across diverse cancer types, influences patient survival as a prognostic biomarker, and modulates drug sensitivity. The strong association of *DHX58* with innate immunity and antiviral response pathways, coupled with its genomic alterations and protein-protein interactions, underscores its critical involvement in cancer biology. While these in silico findings provide valuable insights into *DHX58*'s potential as a therapeutic target and biomarker, further experimental validation through *in vitro* and *in vivo* studies is essential to translate these observations into clinical applications. This research contributes to a deeper understanding of *DHX58*'s multifaceted functions in cancer and paves the way for future investigations into its therapeutic exploitation.

Author Contribution Statement

All authors contributed equally in this study.

Acknowledgements

Ethics Statement

This study was based entirely on publicly available and de-identified datasets, including TCGA, GTEx, CPTAC, and related bioinformatics resources. As no human participants or animals were directly involved, institutional ethics committee approval was not required.

Conflict of Interest

The authors declare that there is no conflict of interest regarding the publication of this manuscript.

References

1. Siegel RL, Miller KD, Wagle NS, Jemal A. Cancer statistics, 2023. CA Cancer J Clin. 2023;73(1):17-48. https://doi.org/10.3322/caac.21763.
2. Hanahan D, Weinberg RA. Hallmarks of cancer: The next generation. Cell. 2011;144(5):646-74. https://doi.org/10.1016/j.cell.2011.02.013.
3. Hanahan D. Hallmarks of cancer: New dimensions. Cancer Discov. 2022;12(1):31-46. https://doi.org/10.1158/2159-8290.Cd-21-1059.
4. Nik-Zainal S. Insights into cancer biology through next-generation sequencing. Clin Med (Lond). 2014;14 Suppl 6:s71-7. https://doi.org/10.7861/clinmedicine.14-6-s71.
5. Jankowsky E, Fairman ME. RNA helicases—one fold for many functions. Current opinion in structural biology. 2007;17(3):316-24.
6. Fuller-Pace FV. Dead box rna helicase functions in cancer. RNA Biol. 2013;10(1):121-32. https://doi.org/10.4161/rna.23312.
7. Rehwinkel J, Gack MU. Rig-i-like receptors: Their regulation and roles in rna sensing. Nat Rev Immunol. 2020;20(9):537-51. https://doi.org/10.1038/s41577-020-0288-3.
8. Pichlmair A, Schulz O, Tan CP, Näslund TI, Liljeström P, Weber F, et al. Rig-i-mediated antiviral responses to single-stranded rna bearing 5'-phosphates. Science. 2006;314(5801):997-1001. https://doi.org/10.1126/science.1132998.
9. Li Y, Zhang L, Wen Z, Wang H, Zhang K, Wang B, et al. Integrative genomic analysis reveals *DHX58* as a key player in gastric cancer. PLoS One. 2026;21(1):e0341230. https://doi.org/10.1371/journal.pone.0341230.
10. Jiang Y, Zhang H, Wang J, Chen J, Guo Z, Liu Y, et al. Exploiting rig-i-like receptor pathway for cancer immunotherapy. J Hematol Oncol. 2023;16(1):8. https://doi.org/10.1186/s13045-023-01405-9.
11. Thul PJ, Lindskog C. The human protein atlas: A spatial map of the human proteome. Protein Sci. 2018;27(1):233-44. https://doi.org/10.1002/pro.3307.
12. Tang Z, Kang B, Li C, Chen T, Zhang Z. Gepia2: An enhanced web server for large-scale expression profiling and interactive analysis. Nucleic Acids Res. 2019;47(W1):W556-w60. https://doi.org/10.1093/nar/gkz430.
13. Li T, Fu J, Zeng Z, Cohen D, Li J, Chen Q, et al. Timer2.0 for analysis of tumor-infiltrating immune cells. Nucleic Acids Res. 2020;48(W1):W509-w14. https://doi.org/10.1093/nar/gkaa407.
14. Chandrashekar DS, Bashel B, Balasubramanya SAH, Creighton CJ, Ponce-Rodriguez I, Chakravarthi B, et al. Ualcan: A portal for facilitating tumor subgroup gene expression and survival analyses. Neoplasia. 2017;19(8):649-58. https://doi.org/10.1016/j.neo.2017.05.002.
15. Li JH, Liu S, Zhou H, Qu LH, Yang JH. Starbase v2.0: Decoding mirna-cerna, mirna-ncrna and protein-rna interaction networks from large-scale clip-seq data. Nucleic Acids Res. 2014;42(Database issue):D92-7. https://doi.org/10.1093/nar/gkt1248.
16. Liu CJ, Hu FF, Xia MX, Han L, Zhang Q, Guo AY. Gscalite: A web server for gene set cancer analysis. Bioinformatics. 2018;34(21):3771-2. https://doi.org/10.1093/bioinformatics/bty411.
17. Liu CJ, Hu FF, Xie GY, Miao YR, Li XW, Zeng Y, et al. Gsca: An integrated platform for gene set cancer analysis at genomic, pharmacogenomic and immunogenomic levels. Brief Bioinform. 2023;24(1). https://doi.org/10.1093/bib/bbac558.
18. Goldman MJ, Craft B, Hastie M, Repečka K, McDade F, Kamath A, et al. Visualizing and interpreting cancer genomics data via the xena platform. Nat Biotechnol. 2020;38(6):675-8. https://doi.org/10.1038/s41587-020-0546-8.
19. Chen EY, Tan CM, Kou Y, Duan Q, Wang Z, Meirelles GV, et al. Enrichr: Interactive and collaborative html5 gene list enrichment analysis tool. BMC Bioinformatics. 2013;14:128. https://doi.org/10.1186/1471-2105-14-128.
20. Xie Z, Bailey A, Kuleshov MV, Clarke DJB, Evangelista JE, Jenkins SL, et al. Gene set knowledge discovery with enrichr. Curr Protoc. 2021;1(3):e90. https://doi.org/10.1002/cpz1.90.
21. Wickham h. Data analysis. Inggplot2: Elegant graphics for data analysis 2016 jun 9 (pp. 189-201). Cham: Springer international publishing.
22. Gao J, Aksoy BA, Dogrusoz U, Dresdner G, Gross B, Sumer SO, et al. Integrative analysis of complex cancer genomics and clinical profiles using the cbioportal. Sci Signal. 2013;6(269):pl1. https://doi.org/10.1126/scisignal.2004088.
23. Szklarczyk D, Gable AL, Nastou KC, Lyon D, Kirsch R, Pyysalo S, et al. The string database in 2021: Customizable protein-protein networks, and functional characterization of user-uploaded gene/measurement sets. Nucleic Acids Res. 2021;49(D1):D605-d12. https://doi.org/10.1093/nar/gkaa1074.
24. Jones PA, Baylin SB. The fundamental role of epigenetic events in cancer. Nat Rev Genet. 2002;3(6):415-28. https://doi.org/10.1038/nrg816.
25. Ding W, Chen J, Feng G, Chen G, Wu J, Guo Y, et al. Dnmivd: DNA methylation interactive visualization database. Nucleic Acids Res. 2020;48(D1):D856-d62. https://doi.org/10.1093/nar/gkz830.
26. Ding W, Feng G, Hu Y, Chen G, Shi T. Co-occurrence and mutual exclusivity analysis of DNA methylation reveals distinct subtypes in multiple cancers. Front Cell Dev Biol. 2020;8:20. https://doi.org/10.3389/fcell.2020.00020.
27. Oliveros jc. Venny. An interactive tool for comparing lists with venn diagrams. (version 2.1). Bioinformatics and evolutionary genomics group, centro nacional de biotecnología (cnb-csic). Available from: Https://bioinfogp.Cnb.Csic.Es/tools/venny/.